ARTICLES

Journal of Semiconductors
(2020) 41, 072906
doi: 10.1088/1674-4926/41/7/072906

Non-volatile optical memory in vertical van der Waals heterostructures

Siyu Zhou[1, 2, 3] and Bo Peng[1, 2, 3, †]

[1]National Engineering Research Center of Electromagnetic Radiation Control Materials, School of Electronic Science and Engineering, University of Electronic Science and Technology of China, Chengdu 611731, China

[2]State Key Laboratory of Electronic Thin Films and Integrated Devices, University of Electronic Science and Technology of China, Chengdu 610054, China

[3]Key Laboratory of Multi-Spectral Absorbing Materials and Structures of Ministry of Education, University of Electronic Science and Technology of China, Chengdu 610054, China

Abstract: Emulating synaptic plasticity in an artificial neural network is crucial to mimic the basic functions of the human brain. In this work, we report a new optoelectronic resistive random access memory (ORRAM) in a three-layer vertical heterostructure of graphene/CdSe quantum dots (QDs)/graphene, which shows non-volatile multi-level optical memory under optical stimuli, giving rise to light-tunable synaptic behaviors. The optical non-volatile storage time is up to ~450 s. The device realizes the function of multi-level optical storage through the interlayer changes between graphene and QDs. This work highlights the feasibility for applying two-dimensional (2D) materials in ORRAM and optoelectronic synaptic devices towards artificial vision.

Key words: ORRAM; heterostructure; synaptic devices

Citation: S Y Zhou and B Peng, Non-volatile optical memory in vertical van der Waals heterostructures[J]. *J. Semicond.*, 2020, 41(7), 072906. http://doi.org/10.1088/1674-4926/41/7/072906

1. Introduction

In the era of big data and artificial intelligence (AI), the demand for processing, memory and communication devices with higher speed, higher efficiency and lower power is becoming ever more urgent[1]. In the conventional von Neumann computing architecture, the memory and processing units are separated and combined together through the electrical interconnection, which lead to high energy consumption and low data transmission speed, and limits the further development of information communication system. Neurons in human brain connected by synapses can process and store great numbers of information simultaneously, which has provided an idea for overcoming the constraint of von Neumann system[2]. Memristive devices exhibit the synaptic behaviors, in which the resistance can be tune by continuous stimuli of voltage or current inputs, showing great potential as memory and logic devices for neuromorphic computing[3–10].

Non-volatile optical memory can directly sense, store, and process optical information in the same way as the neural network in the human visual system with light-tunable plasticity, which opens the door toward low-power artificial vision devices[11]. Two-dimensional (2D) materials have excellent optoelectronic properties, such as strong light-matter interaction[12], large surface-to-volume-ratio[13], reduced screening effect[14, 15] and flexibility. 2D materials open up numerous opportunities for non-volatile devices[16, 17], optical communication[18], imaging sensors[11, 19], logic gates[20], and neuromorphic systems[8]. Graphene modified with the light switchable molecules, azobenzenes, have shown light-driven conductance modulation[21]. However, the photocurrent rising time of ~1000 s is very slow due to the slow transformation of azobenzenes from trans to cis form. To date, there remains a significant challenge on achieving non-volatile optical memory. Herein, we construct a heterstructure geometry comprising graphene and CdSe QDs monolayer to achieve a non-volatile ORRAM device, in which the resistance can be tuned by visible light and exhibits light-tunable synaptic behaviours. The rising time is ~3 s under optical stimuli with a pulse width of 3 s. The optical storage time is up to ~450 s. This work provides a promising non-volatile unit toward neuromorphic systems.

Correspondence to: B Peng, bo_peng@uestc.edu.cn
Received 18 JANUARY 2020; Revised 30 MARCH 2020.

2. Experiment

2.1. Device design

Fig. 1 shows a non-volatile optical memory with three-layer vertical heterostructure of graphene/QDs/graphene on Si/SiO_2 substrate. In the two terminal symmetry ORRAM device, two monolayer graphene are used to sandwich a self-assembled monolayer CdSe QDs[22]. Silver electrodes are connected each piece of graphene (Fig. 1(b)). The CdSe QDs monolayer is used as a light absorption layer to generate photo-induced carriers under light excitation. Under bias voltage, the carriers separate to electrons and holes which disperse to the interface of CdSe QDs and graphene before recombination, in which graphene acts as highways for charge transfer.

2.2. Device fabrication

CVD-grown graphene was spin-coated with PMMA and wet-transferred onto Si/SiO_2 (285 nm) substrate, then acetone was used to remove the PMMA. The monolayer CdSe

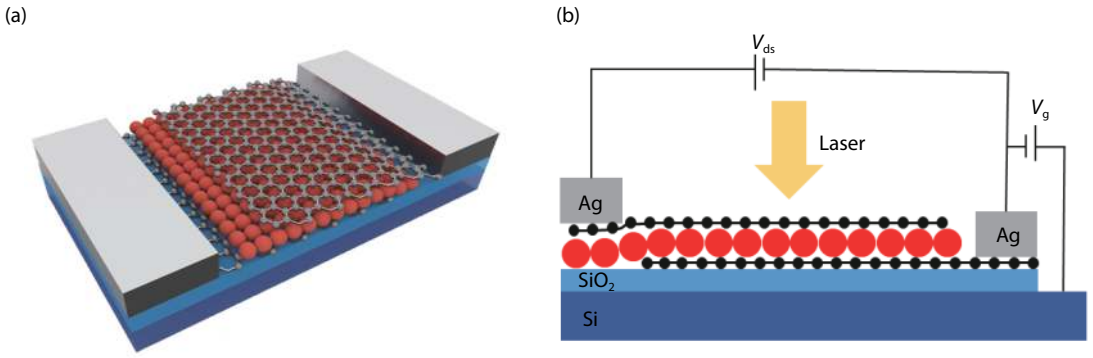

Fig. 1. (Color online) Device schematic. (a) Device with three-layer structure of graphene/CdSe QDs/graphene, silver as the electrodes on each graphene. (b) Circuit connection diagram of the devices.

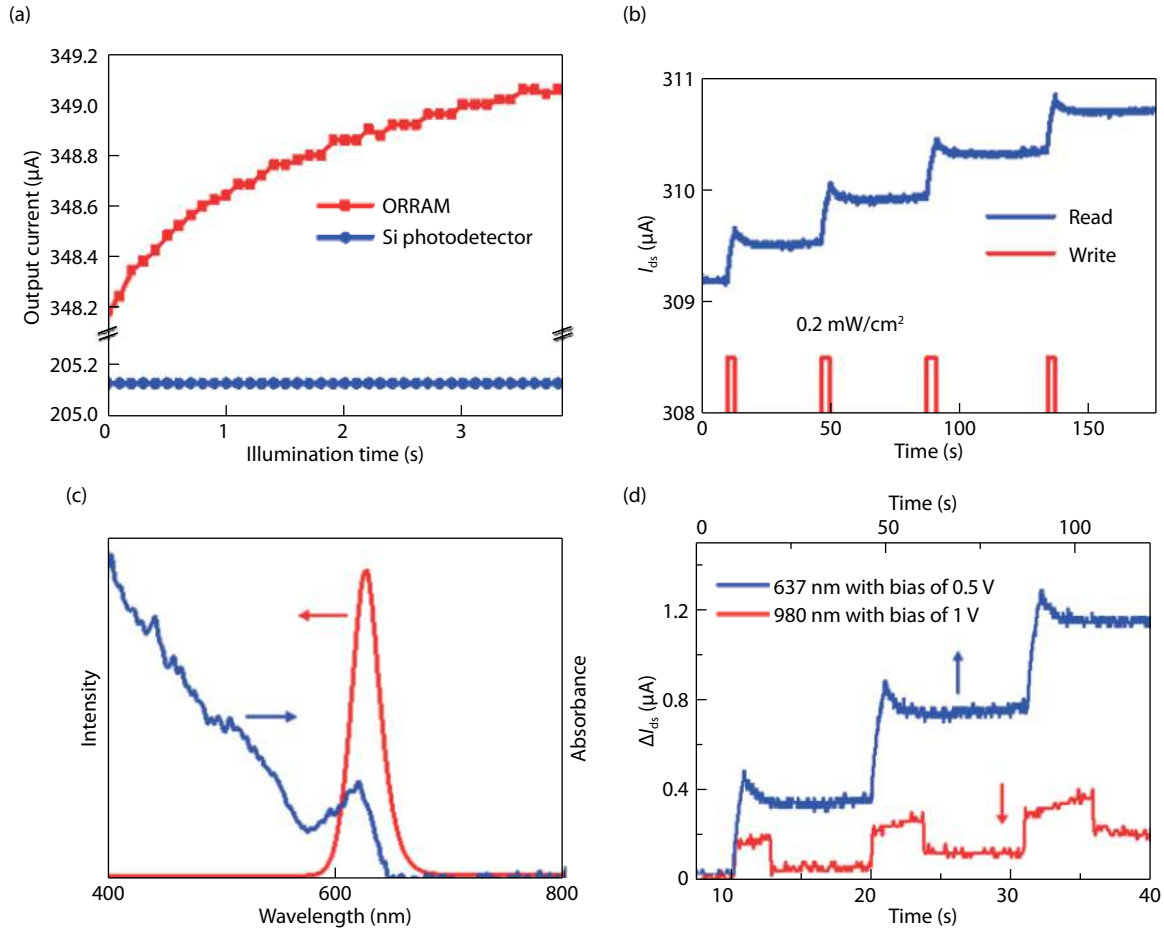

Fig. 2. (Color online) (a) Illumination time dependence of output current of a conventional commercial Si photodetector (blue) and our ORRAM synaptic device (red). (b) The non-volatile optical storage characteristic of the ORRAM device. A laser pulse of 637 nm with 0.2 mW/cm^2 is used to write; a 0.5 V bias is applied to read. The pulse width is 3 s. (c) The absorption and photoluminescence spectra of CdSe QDs. (d) Under the light illumination at 980 and 637 nm, the relative increase of I_{ds} of the device under three laser pulses respectively. Under 637 nm excitation, the photocurrent significantly increase, even the bias is halved.

quantum dot (QD) was prepared by dropping CdSe QDs solution (10 μL) onto the surface of acetonitrile solvent[22]. The self-assembled CdSe QDs monolayer was transferred onto the graphene substrates. Finally, the top graphene was covered on the CdSe QDs monolayer.

3. Results and discussion

The resistance states of the ORRAM device can be tuned by optical stimulation. Displaying time-dependent and light-dosage-dependent behaviors opens the door to emulate the basic features of synaptic plasticity of the human brain. Fig. 2(a) shows the output current of a conventional commercial Si photodetector and our ORRAM synaptic device as a function of the illumination time. The photocurrent of Si photodetector remains constant. However, the output current of the ORRAM device is time-dependent, which increases with increasing illumination time. In many devices, a Schottky barrier may generate built-in electric field, which could drive the

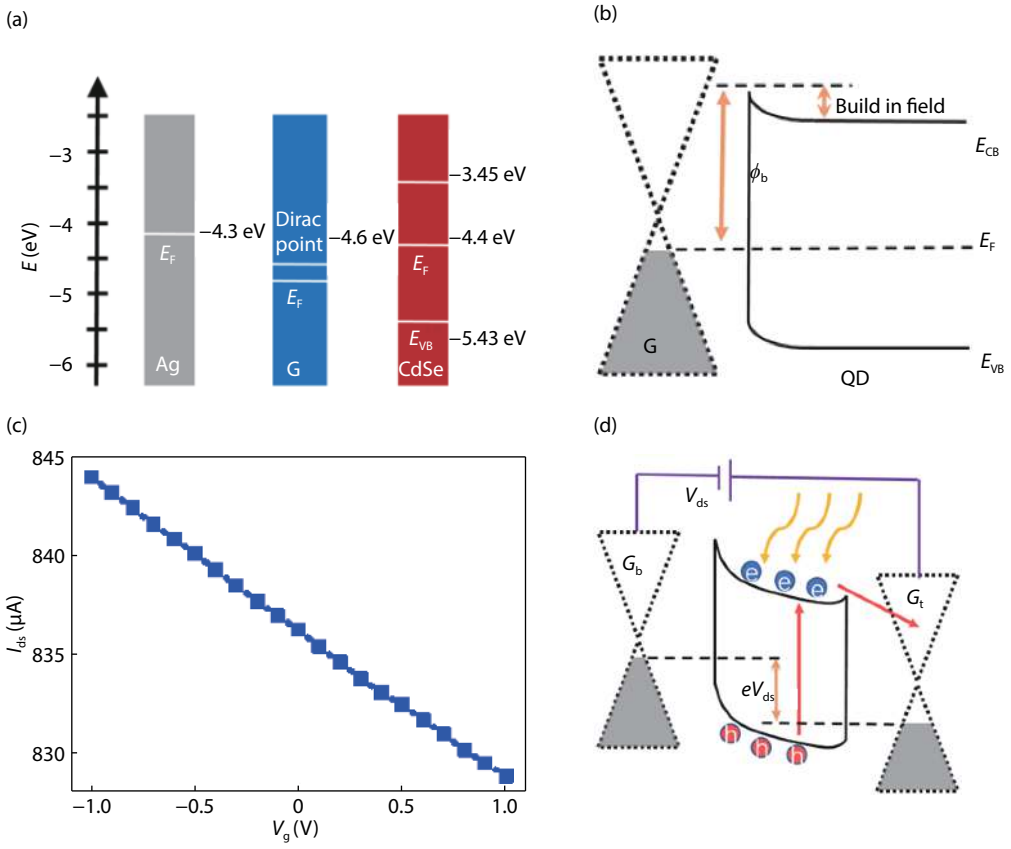

Fig. 3. (Color online) (a) Band offset of Ag, graphene and CdSe QDs. (b) Energy band alignment of graphene and CdSe QDs in the heterojunctions. (c) The gate voltage dependence of I_{ds} under bias of 1 V. (d) Schematic of electrons migration, accumulation and tunneling.

device[23]. But considering the symmetry of our device, the direction of the two layers of Schottky barrier is opposite, so we added bias voltage to drive the device. Fig. 2(b) shows the long-term plasticity under optical stimuli with pulse width of 3 s as a function of pulse number, the laser of 637 nm with 0.2 mW/cm^2 is used as light source. The photocurrent states are preserved after removing the illumination. As the pulse numbers of optical stimulus increase, the output current increases with the same increase magnitude (~0.4 μA/pulse), Thus, the synaptic strengths of the ORRAM device increase significantly.

Fig. 2(c) shows the absorption and photoluminescence spectra of CdSe QDs. The PL peak of CdSe QDs is at ~627 nm and the absorption cutoff wavelength is at ~650 nm, indicating that an illumination wavelength should be smaller than 650 nm to ensure the excitation of QDs layer. In Fig. 2(d), we show the relative increase of the current of the device under three laser pulses. When a laser at 980 nm is used to illuminate the device, the photocurrent dramatically decreases compared with the value upon excitation by 637 nm laser, even both the bias and laser power is increased by 1 time, from 0.5 V and 0.2 mW/cm^2 to 1 V and 0.5 mW/cm^2. Because laser of 980 nm below the absorption cutoff wavelength of QDs, resulting in that the QDs layer does not have any light absorption. The photocurrent under 980 nm excitation arise from the broadband photoresponse of graphene[24]. Carriers are generated after graphene absorbs the photon energy, and could disperse under the bias voltage in the device. The energy band offsets of Ag, graphene and CdSe QDs are shown in Fig. 3(a). The Fermi level of intrinsic graphene and CdSe QDs is about −4.6 and −4.4 eV, respectively. Due to the doping of water vapor and other substances in the air, graphene often shows a p-type doping state, so the Fermi level is lower than the position of Dirac point[25]. The edge of the conduction band (E_{CB}) and valence band (E_{VB}) of the CdSe QDs are located at −3.45 and −5.43 eV, respectively[26]. Because the Fermi level of the CdSe QDs is higher than that of graphene, the band edge (CB and VB) of CdSe QDs thus bend downward at the interface of graphene and CdSe QDs, leading to the formation of the Schottky barrier (Φ_b), as shown in Fig. 3(b). Fig. 3(c) displays the gate dependence of current (I_{ds}) without light illumination under the bias of 1 V. However, it should be noted that this bias dependence of current is measured after the device has been exposed to light for a long time, thus many photogenerated carriers gather in the device, resulting in an increasing absolute current value. When a positive gate voltage is applied ($V_g > 0$), which induce an electron injection, the I_{ds} decrease. In contrast, when we apply $V_g < 0$, the G_b give rise to a hole injection and the I_{ds} increase. This phenomenon validates than a p-type doping can improve the performance of the ORRAM device.

Previous studies have reported defect-induced non-volatile behaviors[27–30], in which charges are trapped by defects like oxygen vacancies, but this could not explain the multi-level storage states of our device. We anticipate that the interfacial Schottky barrier gives rise to the synaptic behaviors. The electrons in CdSe QDs jump to the conduction band from the valence band upon light excitation and leave holes in the valence band. The electrons and holes move in the opposite direction along the tilted band edges arising from the

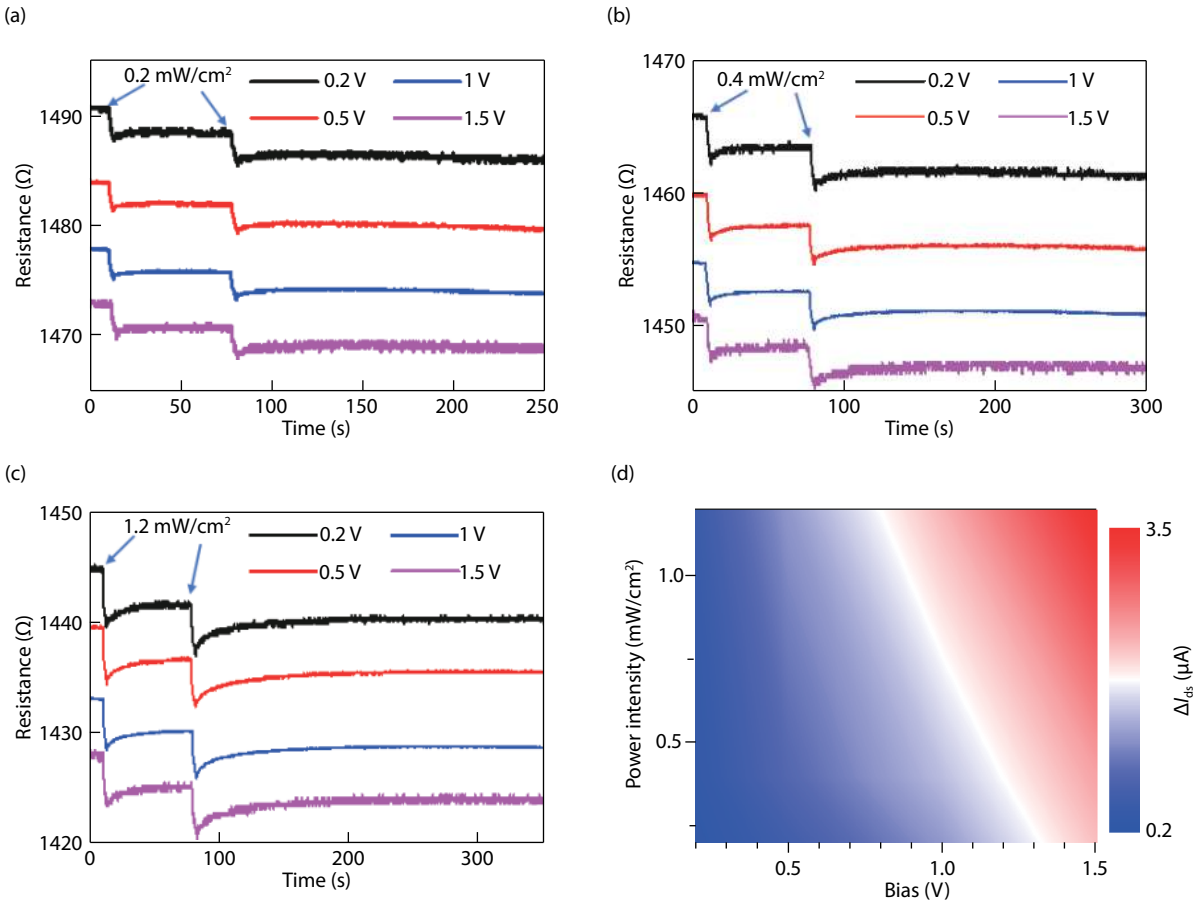

Fig. 4. (Color online) (a–c) The multi-level resistance states of the ORRAM device under different laser power and bias voltages. (d) Corresponding 2D mapping of ΔI_{ds} as a function of bias voltages and laser power.

bias (Fig. 3(d)). The carriers are trapped and accumulate with high densities at the interface of graphene and quantum dots due to the Schottky barrier. Subsequently, the carriers tunnel from the band edges of CdSe QDs to graphene, giving rise to a increasing photocurrent and synaptic behaviors. The non-volatile optical storage time depend on the decay time of the accumulated carriers. Therefore, the output current is dependent on the pulse number of optical stimulus and light dosages.

To further understand the mechanism, the effects of light intensity and bias on the synaptic behaviors are studied. Striking capacities of multi-level storage are observed (Figs. 4(a) and 4(b)). The increased laser power can induce increases of photogenerated carriers gathering at the interface states due to the Schottky barrier, while the increased bias voltage accelerates the carrier migration and tunneling. Thus, the output current and synaptic strengths of the ORRAM devices increase with increasing laser power and bias voltages, consistent with the mechanism in Fig. 3(d). Fig. 4(d) shows the corresponding 2D mapping of the ΔI_{ds}, $\Delta I_{ds} = I_L - I_0$, where I_L and I_0 are the output current in the presence and absence of a pulsed laser illumination, respectively. The non-volatile resistance retention time of the ORRAM device is up to ~450 s after removing bias voltage (Fig. 5), which further confirm the stable long-term plasticity behaviors. The synaptic behaviors of the ORRAM devices can be tuned by light dosage and bias voltages, which allow us to design different strategies to emulate the features of synaptic plasticity to achieve the learning and memory functions of the human brain.

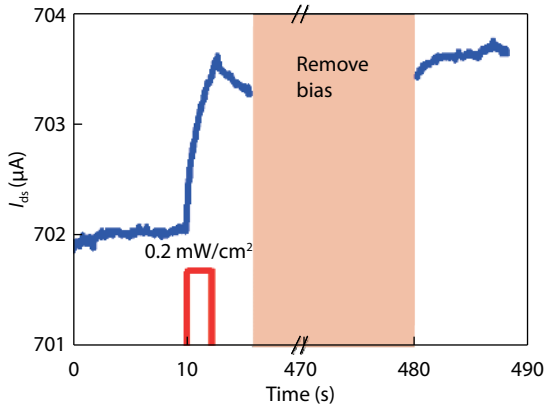

Fig. 5. (Color online) Storage state retention time of the device with bias of 1 V.

4. Conclusion

In this work, we have proposed and demonstrated a non-volatile optical memory and synaptic behaviors in a three-layer vertical heterostructure of graphene/CdSe QDs/graphene. The ORRAM device exhibits multi-level memory capability and long storage time. The Schottky barrier between graphene and CdSe QDs introduces interface states to localize photo-induced carriers, leading to non-volatile optical memory. Furthermore, the low laser power and bias voltage reduce the energy consumption. This work shows great po-

tential to apply 2D heterostructures in non-volatile optical memory and artificial neural networks.

Acknowledgements

We acknowledge financial support from National Science Foundation of China (51602040, 51872039), Science and Technology Program of Sichuan (M112018JY0025) and Scientific Research Foundation for New Teachers of UESTC (A03013023601007).

References

[1] Waldrop M M. The chips are down for Moore's law. Nature, 2016, 530(7589), 144

[2] Indiveri G, Liu S C. Memory and information processing in neuromorphic systems. Proc IEEE, 2015, 103(8), 1379

[3] Cho S, Tan S H, Li Z, et al. SiGe epitaxial memory for neuromorphic computing with reproducible high performance based on engineered dislocations. Nat Mater, 2018, 17(4), 335

[4] Lü J , Chen Y B , Zuo Z, et al. Charge storage characteristics of nonvolatile floating-gate memory based on gradual $Ge_{1-x}Si_x$/Si heteronanocrystals. J Semicond, 2008, 29(4), 770

[5] Zhou H Y, Shi H P, Cheng B C. Surface traps-related nonvolatile resistive switching memory effect in a single SnO_2:Sm nanowire. J Semicond, 2020, 41(1), 012101

[6] Shen J, Cong J, Chai Y, et al. Nonvolatile memory based on nonlinear magnetoelectric effects. Phys Rev Appl, 2016, 6(2), 021001

[7] Shen J, Cong J, Shang D, et al. A multilevel nonvolatile magnetoelectric memory. Sci Rep, 2016, 6, 34473

[8] Jo S H, Chang T, Ebong I, et al. Nanoscale memristor device as synapse in neuromorphic systems. Nano Lett, 2010, 10(4), 1297

[9] Li C, Hu M, Li Y, et al. Analogue signal and image processing with large memristor crossbars. Nat Electron, 2017, 1(1), 52

[10] Zhu D, Li Y, Shen W, et al. Resistive random access memory and its applications in storage and nonvolatile logic. J Semicond, 2017, 38(7), 071002

[11] Zhou F, Zhou Z, Chen J, et al. Optoelectronic resistive random access memory for neuromorphic vision sensors. Nat Nanotechnol, 2019, 14(8), 776

[12] Britnell L, Ribeiro R M, Eckmann A, et al. Strong light-matter interactions in heterostructures of atomically thin films. Science, 2013, 340(6138), 1311

[13] Tran M D, Kim J H, Kim H, et al. Role of hole trap sites in MoS_2 for inconsistency in optical and electrical phenomena. ACS Appl Mater Interfaces, 2018, 10(12), 10580

[14] Yang H, Heo J, Park S, et al. Graphene barristor, a triode device with a gate-controlled Schottky barrier. Science, 2012, 336(6085), 1140

[15] Yu W, Liu Y, Zhou H, et al. Highly efficient gate-tunable photocurrent generation in vertical heterostructures of layered materials. Nat Nanotech, 2013, 8(12), 952

[16] Wang X, Xie W, Xu J B. Graphene based non-volatile memory devices. Adv Mater, 2014, 26(31), 5496

[17] Zhou F, Chen J, Tao X, et al. 2D materials based optoelectronic memory: convergence of electronic memory and optical sensor. Research (Wash D C), 2019, 9490413

[18] Wang Q, Wen Y, Cai K, et al. Nonvolatile infrared memory in MoS_2/PbS van der Waals heterostructures. Sci Adv, 2018, 4(4), 7916

[19] Chen S, Lou Z, Chen D, et al. An artificial flexible visual memory system based on an UV-motivated memristor. Adv Mater, 2018, 30(7), 1705400

[20] Tan H, Liu G, Yang H, et al. Light-gated memristor with integrated logic and memory functions. ACS Nano, 2017, 11(11), 11298

[21] Kang C G, Lee S K, Choe S, et al. Intrinsic photocurrent characteristics of graphene photodetectors passivated with Al_2O_3. Opt Express, 2013, 21(20), 23391

[22] Peng B, Li Z, Mutlugun E, et al. Quantum dots on vertically aligned gold nanorod monolayer: plasmon enhanced fluorescence. Nanoscale, 2014, 6(11), 5592

[23] Qiao H, Huang Z, Ren X, et al. Self-powered photodetectors based on 2D materials. Adv Opt Mater, 2020, 8, 1900765

[24] Zhang B Y, Liu T, Meng B, et al. Broadband high photoresponse from pure monolayer graphene photodetector. Nat Commun, 2013, 4, 1811

[25] Yu Y J, Zhao Y, Ryu S, et al. Tuning the graphene work function by electric field effect. Nano Lett, 2009, 9(10), 3430

[26] Jasieniak J, Califano M, Watkins S E. Size-dependent valence and conduction band-edge energies of semiconductor nanocrystals. ACS Nano, 2011, 5(7), 5888

[27] Zhang Y C, Shao Y Y, Lu X B, et al. Defect states and charge trapping characteristics of HfO_2 films for high performance nonvolatile memory applications. Appl Phys Lett, 2014, 105(17), 113

[28] Cho K, Kim T Y, Park W, et al. Gate-bias stress-dependent photoconductive characteristics of multi-layer MoS_2, field-effect transistors. Nanotechnology, 2014, 25(15), 155201

[29] Bera A, Peng H, Lourembam J, et al. A versatile light-switchable nanorod memory: wurtzite ZnO on perovskite $SrTiO_3$. Adv Funct Mater, 2013, 23(39), 4977

[30] Lee J, Pak S, Lee Y W, et al. Monolayer optical memory cells based on artificial trap-mediated charge storage and release. Nat Commun, 2017, 8, 14734